

# Transplant of microbiota from long-living people to mice reduces aging-related indices and transfers beneficial bacteria

Yinfeng Chen<sup>1</sup>, Siyuan Zhang<sup>1</sup>, Bo Zeng<sup>1</sup>, Jiangchao Zhao<sup>2</sup>, Mingyao Yang<sup>1</sup>, Mingwang Zhang<sup>1</sup>, Yan Li<sup>1</sup>, Qingyong Ni<sup>1</sup>, De Wu<sup>3</sup>, Ying Li<sup>1</sup>

<sup>1</sup>Farm Animal Genetic Resources Exploration and Innovation Key Laboratory of Sichuan Province, Sichuan Agricultural University, Chengdu, Sichuan, China

<sup>2</sup>Department of Animal Science, Division of Agriculture, University of Arkansas, Fayetteville, AR 72701, USA

<sup>3</sup>Institute of Animal Nutrition, Sichuan Agricultural University, Chengdu, Sichuan, China

**Correspondence to:** Ying Li; email: [yingli@sicau.edu.cn](mailto:yingli@sicau.edu.cn)

**Keywords:** longevity, gut microbiota, fecal microbiota transplantation, aging-related index, healthy aging

**Received:** December 20, 2019

**Accepted:** February 20, 2020

**Published:** March 16, 2020

**Copyright:** Chen et al. This is an open-access article distributed under the terms of the Creative Commons Attribution License (CC BY 3.0), which permits unrestricted use, distribution, and reproduction in any medium, provided the original author and source are credited.

## ABSTRACT

A close relationship between age and gut microbiota exists in invertebrates and vertebrates, including humans. Long-living people are a model for studying healthy aging; they also have a distinctive microbiota structure. The relationship between the microbiota of long-living people and aging phenotype remains largely unknown. Herein, the feces of long-living people were transplanted into mice, which were then examined for aging-related indices and beneficial bacteria. Mice transplanted with fecal matter from long-living people (L group) had greater  $\alpha$  diversity, more probiotic genera (*Lactobacillus* and *Bifidobacterium*), and short-chain fatty acid producing genera (*Roseburia*, *Faecalibacterium*, *Ruminococcus*, *Coprococcus*) than the control group. L group mice also accumulated less lipofuscin and  $\beta$ -galactosidase and had longer intestinal villi. This study indicates the effects that the gut microbiota from long-living people have on healthy aging.

## INTRODUCTION

The interactions between gut microbiota and their host(s) have become a popular topic in research. There is growing evidence to suggest that a close relationship exists between gut microbiota and aging [1, 2]. Age-related changes in gut microbiota occur widely among animals, with evidence of this ranging from insects to mammals [3, 4]. Human-based studies have revealed a trend in age-related microbiota features, which shows an increase in gut microbiota diversity from infants to adults, followed by a decrease as adults age [5]. Biagi et al. [6] found signatures of extreme longevity in gut microbiota composition that were related to extreme aging. Combined with the data from Biagi et al. Kong et al. found 11 features shared among long-living Chinese and Italian people, including higher alpha diversity and operational taxonomic units (OTUs) [7]; they also showed that long-living people had greater gut

microbiota diversity than a younger group among Chinese and Japanese populations [8].

High microbiota diversity has been associated with good health in general [9]. Early research on the gut microbiota of elderly people has indicated that healthier subjects have significantly greater gut microbiota diversity than those in long-term residential care [10]. Overall, the information obtained from studies such as these suggests that long-living people can serve as an acceptable model to investigate whether gut microbiota is a feasible target for promoting healthy aging. However, the exact roles that the microbiota play still require investigation.

Studies in animal subjects have shown that age-related microbiota can affect the lifespan of the host [11]. Ten-day-old and 30-day-old *Drosophila* were used as microbiota donors for 10-day-old *Drosophila*. The

lifespan of the 10-day-old transplant group lived significantly longer than the 30-day-old transplant group, and had a decreased frequency in intestinal barrier dysfunction. Subsequently, Smith et al [12] transplanted the gut contents of young and old African turquoise killifish to old fish. Consistent with the results from *Drosophila*, fish transplanted with feces from young donors had a longer lifespan and were significantly more active. These results suggest that the gut microbiota of young individuals can slow host aging and prolong the lifespan of the tested species.

In economically developed countries long-living people (>90 years old) account for approximately 1/5000-1/10000 of the population and usually present good health and mental outlooks, have lower hospitalization rates, and shorter hospitalization times than the general population over their lifetime [13–15]. They also present a delayed onset or absence of senile diseases, such as cardiovascular disease, Alzheimer's disease, and cancer [14, 16, 17]. Previous studies indicate that cancer prevalence in the age groups 60–80 years old range between 25% to 42%, but cancer incidence and cause of death presented a threefold decrease after 90 years old and reached 0–4% above 100 [18]. Therefore, long-living people have been regarded as a suitable model for healthy aging [15]. In the current study, the hypothesis that the gut microbiota of long-living people has the ability to delay host aging compared with those of average lifespan, is tested. To test this hypothesis, the gut microbiota of long-living and typical aging elderly people were transplanted into antibiotic-treated mice, which were then analyzed for differences in gut microbiota and aging indices (Figure 1). L group mice demonstrated greater microbiota diversity and beneficial bacteria, such as probiotic genera and short-chain fatty acid producers. Importantly, aging-related indices, such as lipofuscin and  $\beta$ -galactosidase accumulation, were less in the L group. Our experiment

provided primary evidence that the gut microbiota of long-living people has the ability to delay host aging.

## RESULTS

### Aging-related index assessment

Lipofuscin and  $\beta$ -galactosidase were measured in different tissues of the two groups. Compared to the E group mice, L group mice had significantly lower lipofuscin in the brain tissue (Figure 2A,  $p < 0.05$ ). Similarly, the levels of  $\beta$ -galactosidase in the heart and ileum tissue of L group mice were significantly less than those in the E group mice (Figure 2B and 2C,  $p < 0.0001$ ).

Superoxide dismutase (SOD), glutathione peroxidase (GSH-PX), and malondialdehyde (MDA) in serum were also measured. SOD and GSH-PX activities were not significantly different between L group and E group mice (Supplementary Figure 1A and 1C;  $p = 0.2386$ ;  $0.2597$ , respectively), although activity values from the L group mice tended to be greater. Consistent with this observation, there was no significant difference in MDA levels between the E group and L group mice (Supplementary Figure 1B,  $p = 0.1334$ ).

The intestinal villi of the L group mice were significantly longer than that of the E group mice (Figure 2D,  $p < 0.001$ ), while there was no significant difference in crypt depth between L group and E group mice (Supplementary Figure 1D,  $p = 0.1542$ ).

### 16S rRNA sequence analysis

The change in gut microbiota was analyzed after the transplantation process. Ninety-nine mice fecal samples and two fecal suspensions from long-living and elder donors were collected for 16S rRNA sequencing and

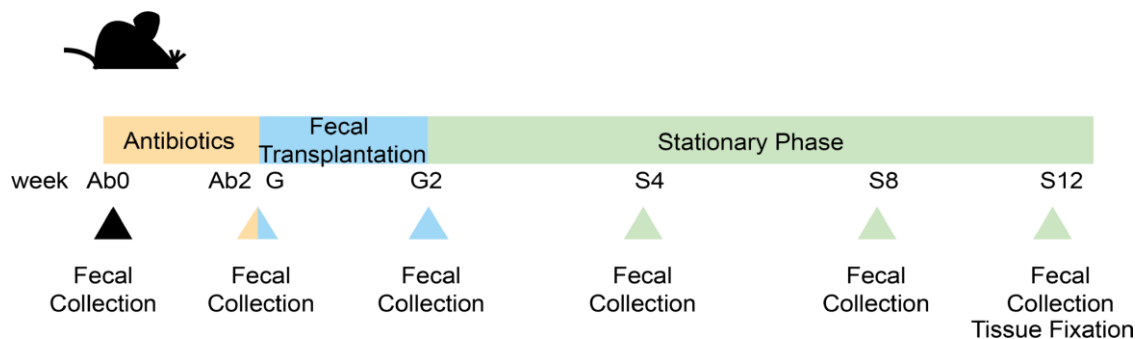


**Figure 1. Experimental design and samples collection.** The whole experiment was divided into 3 phases, totaling 7 sampling points set at the following: before Ab treatment (Ab0); after Ab treatment (Ab2); the first day at FT (G); the last day at FT (G2); 4 weeks after FT (S4); 8 weeks after FT (S8); 12 weeks after FT (S12).

analysis. In total, 6,118,012 high-quality reads corresponding to 22,745 OTUs after filtering for chimeras and low-quality OTUs were identified, which were annotated to 753 genera. Three alpha diversity metrics were calculated to assess the diversity of donors and mice during the whole experiment (Supplementary Figure 2), including Shannon index, Chao1 index, and observed species. As expected, antibiotic treatment significantly decreased the diversity and total bacterial copy number in the mice (Figure 3A, 3B, and Supplementary Figure 3A, 3B,  $p < 0.0001$ ). Unweighted UniFrac distances were used to assess the relationship between the community structure of donors and mice, which was visualized using Principal Coordinates Analysis (PCoA) (Figure 3C). As the number of days increased, donors and recipients clustered together at S12. Alpha diversity increased slightly after the FT (fecal transplantation) phase (G2) and the increasing trend was gradual during the stationary phase (from S4 to S8). Interestingly, the rate of increase in Chao1 diversity was different between the two groups during the FT phase (from G to G2) (Supplementary Figure 2A and 2B). The Chao1 diversity of the L group at G2 was significantly greater than at G (Supplementary Figure 2B,  $p < 0.05$ ). However, there was no significant difference in Chao1 diversity in the E group between G and G2 phase (Supplementary Figure 2A). Consistent

with this result, the alpha diversity of the L group at G2 was significantly greater than that of the E group (Figure 3D and Supplementary Figure 3C, 3D, Chao 1, observed species,  $p < 0.001$ ; Shannon,  $p < 0.05$ ).

### Bacterial genera differences between transplant recipients

LEfSe analysis was used at the genus level to identify the differences in bacterial genera between the E and L groups. Eighty-seven genera were differential in total (Supplementary Figure 4, LDA cut-off = 2,  $p < 0.05$ ). A peak was observed in the number of significantly differential genera in the L group at G2. Forty-two genera were significantly more abundant in the L group than in the E group (Supplementary Figure 4). The relative abundance of *Lactobacillus* at G2 was significantly greater in the L group compared to the E group (Figure 4A,  $p < 0.05$ ); this same trend was observed throughout the entire experiment. The abundance of *Bifidobacterium* was significantly greater in the L group compared to the E group at G2 (Figure 4B,  $p < 0.01$ ).

Six genera that produce short-chain fatty acids (SCFAs) were significantly different between the L and E groups. Of these, four genera (*Roseburia*, *Faecalibacterium*,

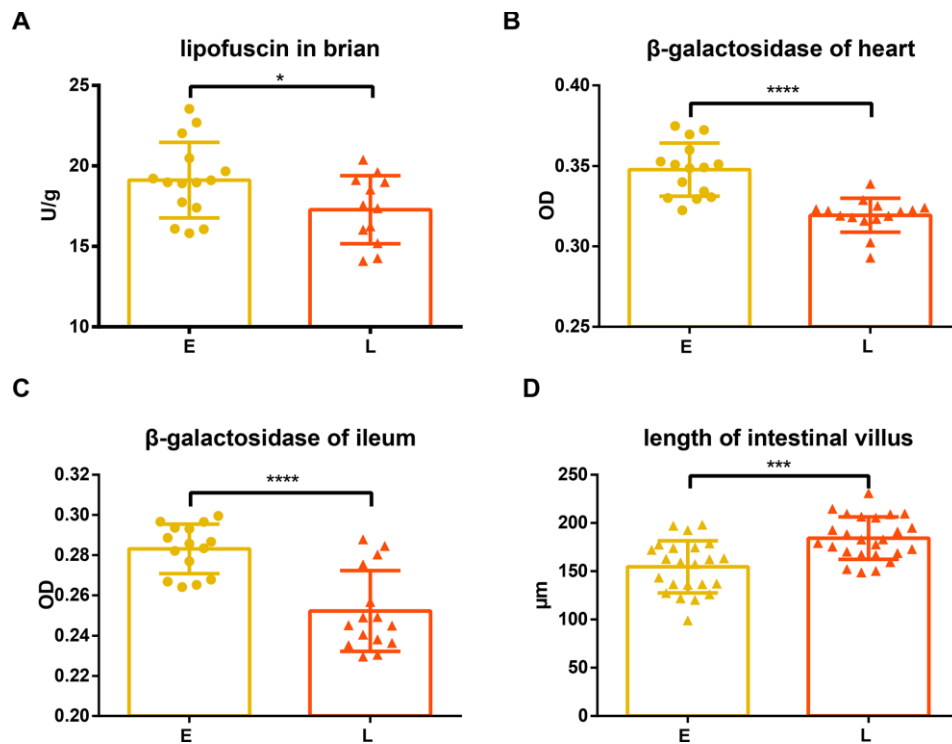


**Figure 2. Difference in aging related indices between groups E and L.** (A) and (D) Lipofuscin in brain and length of intestinal villus are shown on. The level of β-gal in both the (B) heart and (C) ileum in E group and L group. \* $p < 0.05$ , unpaired t test, \*\*\* $p < 0.001$ , \*\*\*\* $p < 0.0001$ , Mann-Whitney U test.

*Ruminococcus*, and *Coprococcus*) at G2 were more abundant in the L group than that in the E group (Figure 4C–4F,  $p < 0.05$ ). Two genera (*Blautia* and *Phascolarctobacterium*) were at S4 more abundant in the E group than that in the L group. (Figure 4G, 4H,  $p < 0.05$ ). Notably, *Bilophila* were significantly abundant in the E group from G2 to S8 than that in the L group (Figure 4I,  $p < 0.01$ ) both at the genus level and OTU level. Cross-referencing data with the NCBI BLAST database led to the annotation of the *Bilophila* species as *Bilophila wadsworthia*.

## DISCUSSION

Thevaranjan et al. demonstrated that age-related alteration of the microbiota can drive age-associated inflammation and intestinal permeability [19]. The intestinal permeability of young germ-free mice was greater when transplanted with the gut microbiota of old mice than when transplanted with that of young mice. Another experiment obtained a similar result in terms of systemic inflammation [20]. Interestingly, Cui et al. found that fecal microbiota transplantation improved the

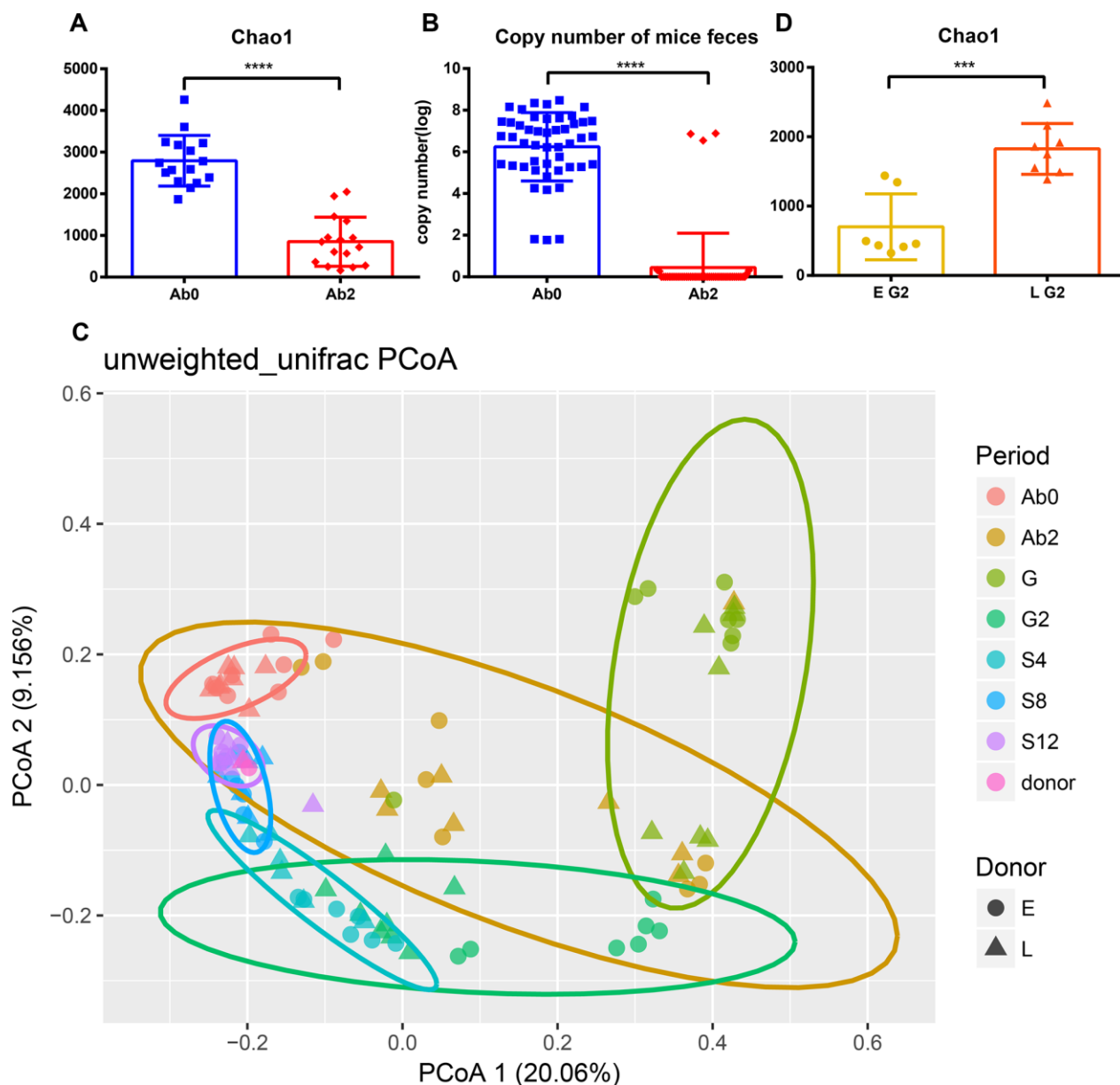


**Figure 3. Efficient antibiotic treatment and transplant.** Antibiotic treatment reduces (A) Chao1 diversity and (B) bacterial copy number. (C) Principal Coordinate Analysis of mice and donor gut microbiomes based on unweighted UniFrac distance. Triangles represent the L group and circles represent the E group. Different colors represent different time periods. (D) The Chao1 diversity of E group and L group after transplantation. \*\*\* $p < 0.001$ , \*\*\*\* $p < 0.0001$ , Mann-Whitney U test.

survival rate of irradiated mice, but microbiota transplantation from older mice failed to improve the survival rate [21]. Together, this evidence suggests that some beneficial component of gut microbiota may be lost with age, or some harmful effects may accumulate. Gut microbiota transplanted from younger donors in *Drosophila melanogaster* and African turquoise killifish have longer lifespans than those who have received transplants from old donors [11, 12]. Studies have shown that there are signatures of extreme longevity in the human gut microbiota, which differ from that of standard aging individuals [2, 6–8]. Therefore, we hypothesize that the gut microbiota from long-living people can slow down aging, which was tested using microbiota transplantation.

Lipofuscin (age pigments) and senescence-associated  $\beta$ -galactosidase have been widely used as biomarkers for aging and replicative senescence, respectively [22–25]. Lipofuscin is an autofluorescent, non-degradable pigment

associated with age, which accumulates because of phagocytosis and autophagocytosis of modified cellular materials within secondary lysosomes of postmitotic cells [22, 26]. The amount of lipofuscin accumulated in neuronal cells increases with age [27, 28] and positively correlates with the production of reactive oxygen species (ROS) and mitochondrial damage [29, 30]. Our results show that lipofuscin accumulated in the brain tissue of L group mice significantly less than in that of E group mice (Figure 2A), suggesting E group mice may have had an increased incidence of oxidative stress, and damaged, defective, impaired, and giant mitochondria with a low rate of degradation [29–33].

Dimri et al. first proposed that  $\beta$ -galactosidase activity that is detectable at pH 6.0 can be defined as senescence-associated  $\beta$ -galactosidase (SA- $\beta$ gal) activity [24]. This has become a well-known biological marker for replicative senescence [34–36]. Experiments have shown that the percentage of SA- $\beta$ gal-positive

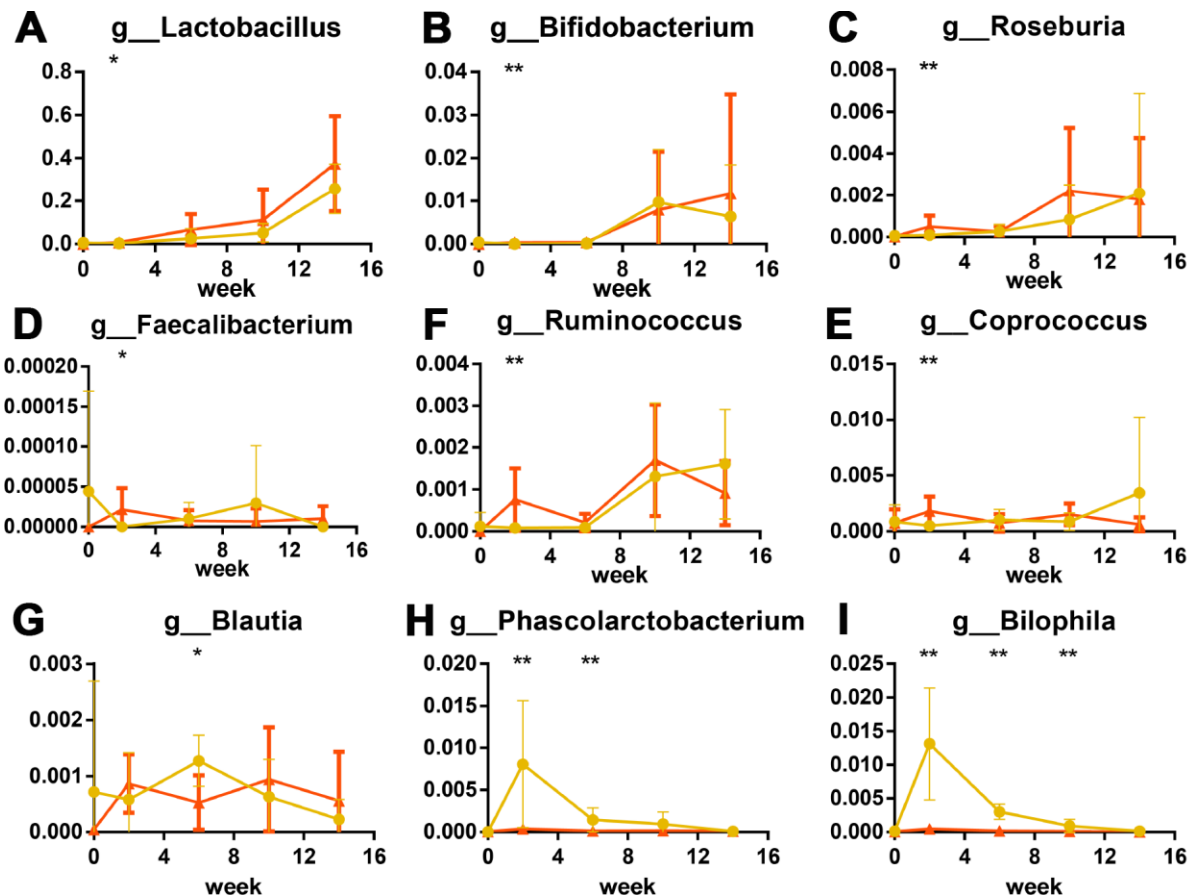


**Figure 4. Significant differences in bacteria in different groups after transplantation (%): Probiotics were significantly greater in abundance in the L group than in E group.** (A) *Lactobacillus*, (B) *Bifidobacterium*. Short chain fatty acid producers were greater in abundance in the L group than in E group are shown as box plots: (C) *Roseburia*, (D) *Faecalibacterium*, (E) *Ruminococcus*, (F) *Coprococcus*. (G) *Phascolarctobacterium* and (H) *Blautia* were more abundant in the E group. The opportunistic pathogen significant higher in E group: *Bilophila wadsworthia* (I) \* $p < 0.05$ , \*\* $p < 0.01$  by LEfSe analysis.



cells was significantly greater in the heart tissue of old mice than that of young mice [37, 38]. However, Kurz et al. demonstrated that SA- $\beta$ gal activity is a sign of residual lysosomal activity at a suboptimal pH, which is detectable due to the increased lysosomal content in senescent cells [39]; they also showed that an increase in SA- $\beta$ gal activity was closely linked to an increase in  $\beta$ -galactosidase protein levels. Another study confirmed that increased SA- $\beta$ gal activity in senescent cells is due at least in part to increased levels of  $\beta$ -galactosidase [40]. Our results showed that the tissues of L group mice accumulated less  $\beta$ -galactosidase than E group mice (Figure 2B and 2C), suggesting that senescent cells accumulated in these tissues had a decreased rate of senescent cells generation or an increased rate of senescent cells clearance in L group mice. In addition, it has been reported that the accumulation of lipofuscin and SA- $\beta$ gal are both associated with lysosomal dysfunction caused by cellular senescence [26, 33, 39, 40]. Therefore, it is likely that fecal microbiota transplantation from long-living people might reduce age-related lysosomal dysfunctions of the recipients because of the reduced lipofuscin and  $\beta$ -galactosidase in the L group mice.

Both SOD and GSH-PX are important antioxidant enzymes to scavenge oxygen free radicals, which cause oxidative damage of cells and correlate with the rate of aging in animals [41–43]. MDA is a product of lipid peroxidation, which reflects the level of cellular oxidative damage [44]. All three indices have been proposed as markers of aging [42]. The SOD and GSH-PX activities were numerically greater whereas the MDA was lower in the L than in the E group mice, suggesting that fecal microbiota transplantation from the long-living people decreased aging related oxidative damage measures (Supplementary Figure 1A–1C). It is worth noting that these measures were only numerically different, but not statistically significant. Future studies with a larger sample size, greater fecal microbiota dosage, and/or longer transplantation duration are desired to reach a statistical significance.

Previous work has indicated that the intestinal capillaries of germ-free mice develop poorly compared to conventional mice, suggesting that the microbiota contributes to the development of intestinal villi [45]. Moreover, the ilea of aged mice were found to exhibit distinct histological features, characterized by a reduction in villus length [46]. We found that the L group mice had longer intestinal villi than those observed in the E group mice (Figure 2D), indicating that the L group has a higher absorptive capacity and younger histological features than the E group.

Together, results from the discussed physiological indices suggest that the gut microbiota from long-

living people could carry an anti-aging function. 16s rRNA results from transplanted mice indicate that the L group mice had more beneficial bacteria (Figure 4). Numerous studies have shown that *Lactobacillus* and *Bifidobacterium* have beneficial effects on diseases such as inflammatory bowel disease, obesity, and type 2 diabetes mellitus [47–50]. Remarkably, *Lactobacillus* and *Bifidobacterium* have been linked to a prolonged lifespan in *Caenorhabditis elegans*, and were found to reduce oxidative stress and lipofuscin accumulation [51, 52]. Exopolysaccharides produced by *Bifidobacterium*, which was isolated from the feces of Chinese centenarians, inhibited lipid peroxidation and reduced lipofuscin accumulation in mouse brain tissue [53]. Overall, the results from these studies are in agreement with our lipofuscin results, and support the hypothesis that the gut microbiota of long-living people can delay host aging more than that of a typical person.

Further analyses used a Linear discriminant analysis (LDA) coupled with effect size (LEfSe) [54] revealed that six SCFA (such as acetate, propionate, and butyrate) producers, which belong to nine predominant genera co-occurred in Chinese healthy young adults [55], enriched in L group mice (*Roseburia*, *Faecalibacterium*, *Ruminococcus* and *Coprococcus*) (Figures 4C–4F) and E group mice (*Blautia*, *Phascolarctobacterium*) (Figures 4G, 4H). SCFAs, especially butyrate, decrease the apoptosis of epithelial cells, and increase the length of intestinal villus in both mice and weaned piglets [56–59]. Butyrate also improves the functions of the intestinal barrier [58, 59], which are related to inflammation [19]. Interestingly, intestinal barrier dysfunction was previously associated with systemic inflammation that shortened the lifespan of *Drosophila melanogaster* [11, 60]. Taken together these results suggest that enriched SCFA producers in the L group mice might contribute to longer intestinal villi and less  $\beta$ -galactosidase. Especially, four SCFAs producers enriched in the L group mice were butyrate-producing bacteria [61–65]. Butyrate was previously linked to increased adhesion of *Lactobacillus* and *Bifidobacterium* to intestine [66], which coincides with the greater abundance of probiotic species in the L group mice mentioned above.

Our LEfSe analysis found that *Bilophila wadsworthia*, which is considered to be an opportunistic pathogen [67] that causes systemic inflammatory response [68, 69], were enriched in the E group mice (Figure 4I). Probiotic species and SCFA producers were previously found to inhibit infection by opportunistic pathogens by niche occupation [66, 70, 71], which could explain why less *Bilophila wadsworthia* were observed in the L group mice.

## Study limitations

Firstly, this study has focused on the effects of gut microbiota transplantation from elder and long-living humans to mice; therefore, further studies using a younger transplant group would be useful for understanding the relationship between age-related gut microbiota and aging. Secondly, a small sample size of 1 donor and 10 recipients per group was used, which means results may be difficult to generalize to a wider population. Huge inter-individual variation has been reported for the human gut microbiota [5, 72]. Hence, our future studies will include larger sample sizes and younger subjects to further explore the role age-related gut microbiota play in aging.

## CONCLUSIONS

In conclusion, results from this study indicate that mice transplanted with gut microbiota from long-living people have more beneficial bacteria and lower metabolites related to aging. This demonstrates the potential use of gut microbiota from long-living people for anti-aging purposes and to promote healthy aging. We also believe that the relationship between aging and gut microbiota is complex. Findings from this study support the hypothesis that age-related microbiota can affect the aging of hosts long-term. Our results provide new insight into healthy aging. Further studies are needed regarding the microbiota's role in long-living people, and also for the role the gut microbiota plays in aging.

## MATERIALS AND METHODS

### Animal study design and treatments

Eleven-month-old male C57BL/6 mice (n=16) were obtained from Chengdu Dossy Experimental Animal Co. Ltd., which were housed in a single cage in a specific pathogen free level animal facility at the Animal Nutrition Institute of Sichuan Agricultural University. All mice were kept under 12/12 hours light/dark cycle and 25 °C and were fed irradiated food and autoclaved water *ad libitum*.

For antibiotic (Ab) treatment, mice were treated for 2 weeks with 1 g/L ampicillin neomycin trisulfate salt hydrate, and metronidazole, and 0.5 g/L vancomycin (Sangon Biotech, Shanghai, China) [73] in their drinking water. After Ab treatment, mice were randomly divided into two groups according to their weight. Fecal matter from the long-living person was transplanted into L group mice and that from the elderly person was transplanted to E group mice. Mice were given 0.2 mL fecal suspension by gavage once a day for

2 weeks. Both volunteers were male, from Dujiangyan, Sichuan province, China, who were both in good health. The long-living person was 101 years old and the elderly person was 70 years old. Human participant ages were divided into two stages according to Odamaki and Biagi's work [5, 6]. Neither had a history of gastrointestinal diseases or record of antibiotic used within 3 months. Feces were collected at the volunteers' homes and put into a sterile fecal collection tube, then transferred to the laboratory within 24 hours in an ice box, and stored at -80 °C immediately. The method of making fecal suspension was slightly adjusted with Turnbaugh's [74]. In brief, suspensions were prepared by diluting 1 g frozen human fecal sample in 10 mL PBS containing 15% glycerol (v/v), under anaerobic conditions. The mixed material was then suspended by vortex, and stored at -80 °C after split charging.

The experimental design, including the time points of sample collection, is shown in Figure 1. Fresh fecal samples were immediately transferred into liquid nitrogen container before they were stored at -80 °C.

### Beta-galactosidase assay

At S12, all mice were anesthetized and killed by cervical dislocation. Heart and ileum tissues were collected for histology by fixing in 4% paraformaldehyde solution overnight. Five-micrometer paraffin sections were processed for immunohistochemistry (IHC) staining and periodic acid Schiff reaction (PAS) staining. For IHC, a primary antibody against beta-galactosidase (Bioss, Beijing, China) was used. The expression level of beta-galactosidase in each tissue was determined by integrated optical density (IOD) and area. The average density (MD) of each microscopic field (objective 400×) was calculated. Five fields PAS stained paraffin sections of ileum tissue were randomly selected and the length of intestinal villi and crypt depths were measured.

### Lipofuscin assay

Lipofuscin concentrations were determined by the lipofuscin extraction method [75]. In short, single mouse brains were homogenized in chloroform-methanol solution (2:1, v/v) to make a 1:20 suspension. An equal volume of distilled water was added, then the solution was mixed using a vortex. After centrifugation at 3000 rpm for 10 min, lipofuscin levels were analyzed from the chloroform phase using a Varioskan LUX Multimode Microplate Reader (Thermo Scientific, USA) based on excitation (360 nm) and emission (420 nm) maxima. Using the fluorescence intensity of quinine sulphate (1 µg/ml) as a unit, the concentration of lipofuscin was expressed in units per g tissue wet weight.

## DNA extraction and bioinformatics

Total bacterial DNA was extracted from fecal samples by using a Magnetic Soil and Stool DNA Kit (TIANGEN Biotech, Beijing, China) according to manufacturer's instruction, and was stored at -80 °C before further analysis. Sequencing was performed at the Novogene Bioinformatics Technology Co., Ltd. Briefly, V3-V4 of the 16S rRNA gene was amplified using the 341F/806R barcode primer pair. All PCR reactions were carried out in 30 µL reactions with 15 µL of Phusion® High-Fidelity PCR Master Mix (New England Biolabs); 0.2 µM of forward and reverse primers, and about 10 ng template DNA. Thermal cycling consisted of initial denaturation at 98 °C for 1 min, followed by 30 cycles of denaturation at 98 °C for 10 s, annealing at 50 °C for 30 s, and elongation at 72 °C for 60 s, with a final 72 °C for 5 min. PCR products were purified using a GeneJET Gel Extraction Kit (Thermo Scientific, USA). Sequencing libraries were generated using a NEB Next® Ultra™ DNA Library Prep Kit for Illumina (NEB, USA) following the manufacturer's recommendations. Amplified libraries were sequenced on an Illumina MiSeq 2 × 250 platform by Novogene (Beijing, China).

Sample reads were assembled by using Qiime software [76]. Chimeric sequences were removed using USEARCH v8.0 [77], and operational taxonomic units (OTUs) were picked de novo with a 97% similarity threshold. Taxonomy assignment of OTUs was performed by comparing sequences to the SILVA database ([http://www.mothur.org/wiki/Silva\\_reference\\_files](http://www.mothur.org/wiki/Silva_reference_files)). Alpha diversity analysis included Shannon index, Chao1, and observed species. Jackknifed beta diversity was represented by unweighted Unifrac distances, calculated with 10 times of subsampling, and these distances were visualized by Principal Coordinate Analysis (PCoA) using R v3.4.3.

## Bacterial quantification by real-time PCR

qPCR analysis of bacterial 16S rRNA copy number was used to quantify the effect of antibiotic treatment. The forward and reverse primers were used as follows: 341F 5'-CCTACGGGAGGCAGCAG-3'; 519R 5'-ATTACCGCGGCTGCTGG-3' [78]. The 10 µL reaction mixture contained 5 µL SYBR® Premix Ex Taq™ II (Takara, Beijing, China), 1 µL DNA (samples or diluted plasmid standards), 0.4 µL (10 µM) of each primer, 3.2 µL ddH<sub>2</sub>O. The PCR program consisted of a DNA denaturation step at 95 °C for 30 s, 40 cycles with an annealing step at 95 °C for 5 s and an elongation step at 60 °C for 30 s. To determine the specificity of amplification, a melting curve was created after the end of amplification.

Standard curves were constructed by PCR product of the 16S rRNA gene of *E.coli*. *E.coli* DH5α genomic DNA was extracted from bacterial liquid using a TIANamp Bacteria DNA Kit (TIANGEN Biotech, Beijing, China). Primers and reaction mixture were used as above, except that SYBR Premix was replaced with Premix Taq™ (Takara, Beijing, China). The PCR program consisted of pre-degeneration at 94 °C for 3 min, 30 cycles with denaturation at 94 °C for 30 s, annealing at 60.6 °C for 30 s, elongation at 72 °C for 30 s and final elongation step at 72 °C for 5 min. PCR products were purified using a Universal DNA Purification Kit (TIANGEN Biotech, Beijing, China). DNA inserts were linked with the pMD19-T vector (Takara, Beijing, China), transformed, plated, and single colonies were selected. Colonies were cultured and plasmids were extracted according to manufacturer's instruction (Takara, Beijing, China) [79]. Plasmids were sequenced to verify successful clones. The concentration of plasmid standard was measured using a spectrophotometer (Thermo Scientific, USA). The target sequence copy number was calculated as previously described [80]. Gradient dilutions were performed to provide a template for the standard curve. The function between threshold cycle (C<sub>t</sub>) and log copy number (x) was  $C_t = -0.3172 * x + 12.289$ , R= 0.9981.

## Statistical analyses

Before significance testing, all data were checked by normal distribution. An Ordinary one-way ANOVA or unpaired t-test were used for significance tests if conforming to a normal distribution, otherwise, a Kruskal-Wallis test or Mann-Whitney test was used. Dunn's multiple comparisons test was used for multiple comparisons. Linear discriminant analysis (LDA) coupled with effect size (LEfSe) [54] was used to identify abundance differential genera or OTUs between groups. GraphPad 6.0 was used for significance testing and visualization. R packages "bindr", "dplyr", "ggpubr", "ggplot2", "vegan", and "reshape2" were used for plotting.

## Ethics approval

This study was approved by the Institutional Animal Care and Use Committee of the Sichuan Agricultural University under the permit number DKY-S20160911. All experiments were performed in accordance with the approved guidelines and regulations.

## AUTHOR CONTRIBUTIONS

Study and experiments were conceived by YL, JZ and YC. YC designed and performed the experiments and



wrote the manuscript. MY, MZ, Yan Li, QN, DW contributed reagents, materials and histology analysis tools. YC, SZ and BZ contributed to the analysis of data.

## CONFLICTS OF INTEREST

The authors declare that they have no conflicts of interests.

## FUNDING

This work was supported by the National Natural Science Foundation of China (31471997) to YL.

## REFERENCES

1. Heintz C, Mair W. You are what you host: microbiome modulation of the aging process. *Cell*. 2014; 156:408–11.  
<https://doi.org/10.1016/j.cell.2014.01.025>  
PMID:[24485451](https://pubmed.ncbi.nlm.nih.gov/24485451/)
2. Biagi E, Rampelli S, Turrone S, Quercia S, Candela M, Brigidi P. The gut microbiota of centenarians: signatures of longevity in the gut microbiota profile. *Mech Ageing Dev*. 2017; 165:180–84.  
<https://doi.org/10.1016/j.mad.2016.12.013>  
PMID:[28049008](https://pubmed.ncbi.nlm.nih.gov/28049008/)
3. Han G, Lee HJ, Jeong SE, Jeon CO, Hyun S. Comparative Analysis of *Drosophila melanogaster* Gut Microbiota with Respect to Host Strain, Sex, and Age. *Microb Ecol*. 2017; 74:207–16.  
<https://doi.org/10.1007/s00248-016-0925-3>  
PMID:[28054304](https://pubmed.ncbi.nlm.nih.gov/28054304/)
4. Langille MG, Meehan CJ, Koenig JE, Dhanani AS, Rose RA, Howlett SE, Beiko RG. Microbial shifts in the aging mouse gut. *Microbiome*. 2014; 2:50.  
<https://doi.org/10.1186/s40168-014-0050-9>  
PMID:[25520805](https://pubmed.ncbi.nlm.nih.gov/25520805/)
5. Odamaki T, Kato K, Sugahara H, Hashikura N, Takahashi S, Xiao J, Abe F, Osawa R. Age-related changes in gut microbiota composition from newborn to centenarian: a cross-sectional study. *BMC Microbiol*. 2016; 16:90.  
<https://doi.org/10.1186/s12866-016-0708-5>  
PMID:[27220822](https://pubmed.ncbi.nlm.nih.gov/27220822/)
6. Biagi E, Franceschi C, Rampelli S, Severgnini M, Ostan R, Turrone S, Consolandi C, Quercia S, Scurti M, Monti D, Capri M, Brigidi P, Candela M. Gut Microbiota and Extreme Longevity. *Curr Biol*. 2016; 26:1480–85.  
<https://doi.org/10.1016/j.cub.2016.04.016>  
PMID:[27185560](https://pubmed.ncbi.nlm.nih.gov/27185560/)
7. Kong F, Hua Y, Zeng B, Ning R, Li Y, Zhao J. Gut microbiota signatures of longevity. *Curr Biol*. 2016; 26:R832–33.  
<https://doi.org/10.1016/j.cub.2016.08.015>  
PMID:[27676296](https://pubmed.ncbi.nlm.nih.gov/27676296/)
8. Kong F, Deng F, Li Y, Zhao J. Identification of gut microbiome signatures associated with longevity provides a promising modulation target for healthy aging. *Gut Microbes*. 2019; 10:210–15.  
<https://doi.org/10.1080/19490976.2018.1494102>  
PMID:[30142010](https://pubmed.ncbi.nlm.nih.gov/30142010/)
9. Lloyd-Price J, Abu-Ali G, Huttenhower C. The healthy human microbiome. *Genome Med*. 2016; 8:51.  
<https://doi.org/10.1186/s13073-016-0307-y>  
PMID:[27122046](https://pubmed.ncbi.nlm.nih.gov/27122046/)
10. Claesson MJ, Jeffery IB, Conde S, Power SE, O'Connor EM, Cusack S, Harris HM, Coakley M, Lakshminarayanan B, O'Sullivan O, Fitzgerald GF, Deane J, O'Connor M, et al. Gut microbiota composition correlates with diet and health in the elderly. *Nature*. 2012; 488:178–84.  
<https://doi.org/10.1038/nature11319> PMID:[22797518](https://pubmed.ncbi.nlm.nih.gov/22797518/)
11. Clark RI, Salazar A, Yamada R, Fitz-Gibbon S, Morselli M, Alcaraz J, Rana A, Rera M, Pellegrini M, Ja WW, Walker DW. Distinct Shifts in Microbiota Composition during *Drosophila* Aging Impair Intestinal Function and Drive Mortality. *Cell Rep*. 2015; 12:1656–67.  
<https://doi.org/10.1016/j.celrep.2015.08.004>  
PMID:[26321641](https://pubmed.ncbi.nlm.nih.gov/26321641/)
12. Smith P, Willemsen D, Popkes M, Metge F, Gandiwa E, Reichard M, Valenzano DR. Regulation of life span by the gut microbiota in the short-lived African turquoise killifish. *eLife*. 2017; 6:6.  
<https://doi.org/10.7554/eLife.27014> PMID:[28826469](https://pubmed.ncbi.nlm.nih.gov/28826469/)
13. Engberg H, Oksuzyan A, Jeune B, Vaupel JW, Christensen K. Centenarians—a useful model for healthy aging? A 29-year follow-up of hospitalizations among 40,000 Danes born in 1905. *Aging Cell*. 2009; 8:270–76.  
<https://doi.org/10.1111/j.1474-9726.2009.00474.x>  
PMID:[19627266](https://pubmed.ncbi.nlm.nih.gov/19627266/)
14. Hitt R, Young-Xu Y, Silver M, Perls T. Centenarians: the older you get, the healthier you have been. *Lancet*. 1999; 354:652.  
[https://doi.org/10.1016/S0140-6736\(99\)01987-X](https://doi.org/10.1016/S0140-6736(99)01987-X)  
PMID:[10466675](https://pubmed.ncbi.nlm.nih.gov/10466675/)
15. Galioto A, Dominguez LJ, Pineo A, Ferlisi A, Putignano E, Belvedere M, Costanza G, Barbagallo M. Cardiovascular risk factors in centenarians. *Exp Gerontol*. 2008; 43:106–13.  
<https://doi.org/10.1016/j.exger.2007.06.009>  
PMID:[17689040](https://pubmed.ncbi.nlm.nih.gov/17689040/)
16. Selim AJ, Fincke G, Berlowitz DR, Miller DR, Qian SX, Lee A, Cong Z, Rogers W, Selim BJ, Ren XS, Spiro A 3rd, Kazis LE. Comprehensive health status assessment of

- centenarians: results from the 1999 large health survey of veteran enrollees. *J Gerontol A Biol Sci Med Sci*. 2005; 60:515–19.  
<https://doi.org/10.1093/gerona/60.4.515>  
PMID:15933394
17. Pavlidis N, Stanta G, Audisio RA. Cancer prevalence and mortality in centenarians: a systematic review. *Crit Rev Oncol Hematol*. 2012; 83:145–52.  
<https://doi.org/10.1016/j.critrevonc.2011.09.007>  
PMID:22024388
18. Franceschi C, Bonafè M. Centenarians as a model for healthy aging. *Biochem Soc Trans*. 2003; 31:457–61.  
<https://doi.org/10.1042/bst0310457> PMID:12653662
19. Thevaranjan N, Puchta A, Schulz C, Naidoo A, Szamosi JC, Verschoor CP, Loukov D, Schenck LP, Jury J, Foley KP, Schertzer JD, Larché MJ, Davidson DJ, et al. Age-Associated Microbial Dysbiosis Promotes Intestinal Permeability, Systemic Inflammation, and Macrophage Dysfunction. *Cell Host Microbe*. 2017; 21:455–466.e4.  
<https://doi.org/10.1016/j.chom.2017.03.002>  
PMID:28407483
20. Fransen F, van Beek AA, Borghuis T, Aidy SE, Hugenholtz F, van der Gaast-de Jongh C, Savelkoul HF, De Jonge MI, Boekschoten MV, Smidt H, Faas MM, de Vos P. Aged Gut Microbiota Contributes to Systemical Inflammation after Transfer to Germ-Free Mice. *Front Immunol*. 2017; 8:1385.  
<https://doi.org/10.3389/fimmu.2017.01385>  
PMID:29163474
21. Cui M, Xiao H, Li Y, Zhou L, Zhao S, Luo D, Zheng Q, Dong J, Zhao Y, Zhang X, Zhang J, Lu L, Wang H, Fan S. Faecal microbiota transplantation protects against radiation-induced toxicity. *EMBO Mol Med*. 2017; 9:448–61.  
<https://doi.org/10.15252/emmm.201606932>  
PMID:28242755
22. Yin D. Biochemical basis of lipofuscin, ceroid, and age pigment-like fluorophores. *Free Radic Biol Med*. 1996; 21:871–88.  
[https://doi.org/10.1016/0891-5849\(96\)00175-X](https://doi.org/10.1016/0891-5849(96)00175-X)  
PMID:8902532
23. Ikeda H, Tauchi H, Shimasaki H, Ueta N, Sato T. Age and organ difference in amount and distribution of autofluorescent granules in rats. *Mech Ageing Dev*. 1985; 31:139–46.  
[https://doi.org/10.1016/S0047-6374\(85\)80024-5](https://doi.org/10.1016/S0047-6374(85)80024-5)  
PMID:4058065
24. Dimri GP, Lee X, Basile G, Acosta M, Scott G, Roskelley C, Medrano EE, Linskens M, Rubelj I, Pereira-Smith O, Et A. A biomarker that identifies senescent human cells in culture and in aging skin in vivo. *Proc Natl Acad Sci USA*. 1995; 92:9363–67.  
<https://doi.org/10.1073/pnas.92.20.9363>  
PMID:7568133
25. López-Otín C, Blasco MA, Partridge L, Serrano M, Kroemer G. The hallmarks of aging. *Cell*. 2013; 153:1194–217.  
<https://doi.org/10.1016/j.cell.2013.05.039>  
PMID:23746838
26. Jung T, Bader N, Grune T. Lipofuscin: formation, distribution, and metabolic consequences. *Ann N Y Acad Sci*. 2007; 1119:97–111.  
<https://doi.org/10.1196/annals.1404.008>  
PMID:18056959
27. Nakano M, Oenzil F, Mizuno T, Gotoh S. Age-related changes in the lipofuscin accumulation of brain and heart. *Gerontology*. 1995 (Suppl 2); 41:69–79.  
<https://doi.org/10.1159/000213726> PMID:8821322
28. Double KL, Dedov VN, Fedorow H, Kettle E, Halliday GM, Garner B, Brunk UT. The comparative biology of neuromelanin and lipofuscin in the human brain. *Cell Mol Life Sci*. 2008; 65:1669–82.  
<https://doi.org/10.1007/s00018-008-7581-9>  
PMID:18278576
29. Terman A, Dalen H, Eaton JW, Neuzil J, Brunk UT. Aging of cardiac myocytes in culture: oxidative stress, lipofuscin accumulation, and mitochondrial turnover. *Ann N Y Acad Sci*. 2004; 1019:70–77.  
<https://doi.org/10.1196/annals.1297.015>  
PMID:15246997
30. von Zglinicki T, Nilsson E, Döcke WD, Brunk UT. Lipofuscin accumulation and ageing of fibroblasts. *Gerontology*. 1995 (Suppl 2); 41:95–108.  
<https://doi.org/10.1159/000213728> PMID:8821324
31. Riga D, Riga S, Halalau F, Schneider F. Brain lipopigment accumulation in normal and pathological aging. *Ann N Y Acad Sci*. 2006; 1067:158–63.  
<https://doi.org/10.1196/annals.1354.019>  
PMID:16803981
32. Moreno-García A, Kun A, Calero O, Medina M, Calero M. An Overview of the Role of Lipofuscin in Age-Related Neurodegeneration. *Front Neurosci*. 2018; 12:464.  
<https://doi.org/10.3389/fnins.2018.00464>  
PMID:30026686
33. Brunk UT, Terman A. Lipofuscin: mechanisms of age-related accumulation and influence on cell function. *Free Radic Biol Med*. 2002; 33:611–19.  
[https://doi.org/10.1016/S0891-5849\(02\)00959-0](https://doi.org/10.1016/S0891-5849(02)00959-0)  
PMID:12208347
34. Melk A, Kittikowit W, Sandhu I, Halloran KM, Grimm P, Schmidt BM, Halloran PF. Cell senescence in rat kidneys in vivo increases with growth and age despite

- lack of telomere shortening. *Kidney Int.* 2003; 63:2134–43.  
<https://doi.org/10.1046/j.1523-1755.2003.00032.x>  
PMID:12753300
35. Pendergrass WR, Lane MA, Bodkin NL, Hansen BC, Ingram DK, Roth GS, Yi L, Bin H, Wolf NS. Cellular proliferation potential during aging and caloric restriction in rhesus monkeys (*Macaca mulatta*). *J Cell Physiol.* 1999; 180:123–30.  
[https://doi.org/10.1002/\(SICI\)1097-4652\(199907\)180:1<123::AID-JCP14>3.0.CO;2-W](https://doi.org/10.1002/(SICI)1097-4652(199907)180:1<123::AID-JCP14>3.0.CO;2-W)  
PMID:10362025
36. Spazzafumo L, Mensà E, Matacchione G, Galeazzi T, Zampini L, Recchioni R, Marcheselli F, Prattichizzo F, Testa R, Antonicelli R, Garagnani P, Boemi M, Bonafè M, et al. Age-related modulation of plasmatic beta-Galactosidase activity in healthy subjects and in patients affected by T2DM. *Oncotarget.* 2017; 8:93338–48.  
<https://doi.org/10.18632/oncotarget.21848>  
PMID:29212153
37. Maejima Y, Adachi S, Ito H, Hirao K, Isobe M. Induction of premature senescence in cardiomyocytes by doxorubicin as a novel mechanism of myocardial damage. *Aging Cell.* 2008; 7:125–36.  
<https://doi.org/10.1111/j.1474-9726.2007.00358.x>  
PMID:18031568
38. Inuzuka Y, Okuda J, Kawashima T, Kato T, Niizuma S, Tamaki Y, Iwanaga Y, Yoshida Y, Kosugi R, Watanabe-Maeda K, Machida Y, Tsuji S, Aburatani H, et al. Suppression of phosphoinositide 3-kinase prevents cardiac aging in mice. *Circulation.* 2009; 120:1695–703.  
<https://doi.org/10.1161/CIRCULATIONAHA.109.871137>  
PMID:19822807
39. Kurz DJ, Decary S, Hong Y, Erusalimsky JD. Senescence-associated (beta)-galactosidase reflects an increase in lysosomal mass during replicative ageing of human endothelial cells. *J Cell Sci.* 2000; 113:3613–22.  
PMID:11017877
40. Lee BY, Han JA, Im JS, Morrone A, Johung K, Goodwin EC, Kleijer WJ, DiMaio D, Hwang ES. Senescence-associated  $\beta$ -galactosidase is lysosomal  $\beta$ -galactosidase. *Aging Cell.* 2006; 5:187–95.  
<https://doi.org/10.1111/j.1474-9726.2006.00199.x>  
PMID:16626397
41. Barja G. Rate of generation of oxidative stress-related damage and animal longevity. *Free Radic Biol Med.* 2002; 33:1167–72.  
[https://doi.org/10.1016/S0891-5849\(02\)00910-3](https://doi.org/10.1016/S0891-5849(02)00910-3)  
PMID:12398924
42. Martínez de Toda I, Vida C, Sanz San Miguel L, De la Fuente M. Function, Oxidative, and Inflammatory Stress Parameters in Immune Cells as Predictive Markers of Lifespan throughout Aging. *Oxid Med Cell Longev.* 2019; 2019:4574276.  
<https://doi.org/10.1155/2019/4574276>  
PMID:31281577
43. Maurya PK, Noto C, Rizzo LB, Rios AC, Nunes SO, Barbosa DS, Sethi S, Zeni M, Mansur RB, Maes M, Brietzke E. The role of oxidative and nitrosative stress in accelerated aging and major depressive disorder. *Prog Neuropsychopharmacol Biol Psychiatry.* 2016; 65:134–44.  
<https://doi.org/10.1016/j.pnpbp.2015.08.016>  
PMID:26348786
44. Kwiecien S, Jasnos K, Magierowski M, Sliwowski Z, Pajdo R, Brzozowski B, Mach T, Wojcik D, Brzozowski T. Lipid peroxidation, reactive oxygen species and antioxidative factors in the pathogenesis of gastric mucosal lesions and mechanism of protection against oxidative stress - induced gastric injury. *J Physiol Pharmacol.* 2014; 65:613–22. PMID:25371520
45. Hooper LV. Bacterial contributions to mammalian gut development. *Trends Microbiol.* 2004; 12:129–34.  
<https://doi.org/10.1016/j.tim.2004.01.001>  
PMID:15001189
46. Tremblay S, Côté NM, Grenier G, Duclos-Lasnier G, Fortier LC, Ilangumaran S, Menendez A. Ileal antimicrobial peptide expression is dysregulated in old age. *Immun Ageing.* 2017; 14:19.  
<https://doi.org/10.1186/s12979-017-0101-8>  
PMID:28855949
47. Plaza-Díaz J, Ruiz-Ojeda FJ, Vilchez-Padial LM, Gil A. Evidence of the Anti-Inflammatory Effects of Probiotics and Synbiotics in Intestinal Chronic Diseases. *Nutrients.* 2017; 9:555.  
<https://doi.org/10.3390/nu9060555>  
PMID:28555037
48. John GK, Wang L, Nanavati J, Twose C, Singh R, Mullin G. Dietary Alteration of the Gut Microbiome and Its Impact on Weight and Fat Mass: A Systematic Review and Meta-Analysis. *Genes (Basel).* 2018; 9:167.  
<https://doi.org/10.3390/genes9030167>  
PMID:29547587
49. Zhang Q, Wu Y, Fei X. Effect of probiotics on glucose metabolism in patients with type 2 diabetes mellitus: A meta-analysis of randomized controlled trials. *Medicina (Kaunas).* 2016; 52:28–34.  
<https://doi.org/10.1016/j.medici.2015.11.008>  
PMID:26987497
50. Sabico S, Al-Mashharawi A, Al-Daghri NM, Wani K, Amer OE, Hussain DS, Ahmed Ansari MG, Masoud MS, Alokail MS, McTernan PG. Effects of a 6-month multi-strain probiotics supplementation in endotoxemic,

- inflammatory and cardiometabolic status of T2DM patients: A randomized, double-blind, placebo-controlled trial. *Clin Nutr.* 2019; 38:1561–69. <https://doi.org/10.1016/j.clnu.2018.08.009> PMID:30170781
51. Komura T, Ikeda T, Yasui C, Saeki S, Nishikawa Y. Mechanism underlying longevity induced by bifidobacteria in *Caenorhabditis elegans*. *Biogerontology.* 2013; 14:73–87. <https://doi.org/10.1007/s10522-012-9411-6> PMID:23291976
  52. Grompone G, Martorell P, Llopis S, González N, Genovés S, Mulet AP, Fernández-Calero T, Tiscornia I, Bollati-Fogolin M, Chambaud I, Foligné B, Montserrat A, Ramón D. Anti-inflammatory *Lactobacillus rhamnosus* CNCM I-3690 strain protects against oxidative stress and increases lifespan in *Caenorhabditis elegans*. *PLoS One.* 2012; 7:e52493. <https://doi.org/10.1371/journal.pone.0052493> PMID:23300685
  53. Xu R, Shang N, Li P. In vitro and in vivo antioxidant activity of exopolysaccharide fractions from *Bifidobacterium animalis* RH. *Anaerobe.* 2011; 17:226–31. <https://doi.org/10.1016/j.anaerobe.2011.07.010> PMID:21875680
  54. Segata N, Izard J, Waldron L, Gevers D, Miropolsky L, Garrett WS, Huttenhower C. Metagenomic biomarker discovery and explanation. *Genome Biol.* 2011; 12:R60. <https://doi.org/10.1186/gb-2011-12-6-r60> PMID:21702898
  55. Zhang J, Guo Z, Xue Z, Sun Z, Zhang M, Wang L, Wang G, Wang F, Xu J, Cao H, Xu H, Lv Q, Zhong Z, et al. A phylo-functional core of gut microbiota in healthy young Chinese cohorts across lifestyles, geography and ethnicities. *ISME J.* 2015; 9:1979–90. <https://doi.org/10.1038/ismej.2015.11> PMID:25647347
  56. Diao H. Effects of Gut Microbiota and SCFAs on Intestinal Structure and Functions of Pigs and the Underlying Mechanisms. Sichuan Agricultural University, Animal Nutrition Institute; 2016.
  57. Hass R, Busche R, Luciano L, Reale E, Engelhardt WV. Lack of butyrate is associated with induction of Bax and subsequent apoptosis in the proximal colon of guinea pig. *Gastroenterology.* 1997; 112:875–81. <https://doi.org/10.1053/gast.1997.v112.pm9041249> PMID:9041249
  58. Han X, Song H, Wang Y, Sheng Y, Chen J. Sodium butyrate protects the intestinal barrier function in peritonitic mice. *Int J Clin Exp Med.* 2015; 8:4000–07. PMID:26064302
  59. Diao H, Jiao AR, Yu B, Mao XB, Chen DW. Gastric infusion of short-chain fatty acids can improve intestinal barrier function in weaned piglets. *Genes Nutr.* 2019; 14:4. <https://doi.org/10.1186/s12263-019-0626-x> PMID:30761185
  60. Rera M, Clark RI, Walker DW. Intestinal barrier dysfunction links metabolic and inflammatory markers of aging to death in *Drosophila*. *Proc Natl Acad Sci USA.* 2012; 109:21528–33. <https://doi.org/10.1073/pnas.1215849110> PMID:23236133
  61. Pryde SE, Duncan SH, Hold GL, Stewart CS, Flint HJ. The microbiology of butyrate formation in the human colon. *FEMS Microbiol Lett.* 2002; 217:133–39. <https://doi.org/10.1111/j.1574-6968.2002.tb11467.x> PMID:12480096
  62. Duncan SH, Hold GL, Harmsen HJ, Stewart CS, Flint HJ. Growth requirements and fermentation products of *Fusobacterium prausnitzii*, and a proposal to reclassify it as *Faecalibacterium prausnitzii* gen. nov., comb. nov. *Int J Syst Evol Microbiol.* 2002; 52:2141–46. <https://doi.org/10.1099/00207713-52-6-2141> PMID:12508881
  63. Duncan SH, Aminov RI, Scott KP, Louis P, Stanton TB, Flint HJ. Proposal of *Roseburia faecis* sp. nov., *Roseburia hominis* sp. nov. and *Roseburia inulinivorans* sp. nov., based on isolates from human faeces. *Int J Syst Evol Microbiol.* 2006; 56:2437–41. <https://doi.org/10.1099/ijs.0.64098-0> PMID:17012576
  64. Liu C, Finegold SM, Song Y, Lawson PA. Reclassification of *Clostridium coccoides*, *Ruminococcus hansenii*, *Ruminococcus hydrogenotrophicus*, *Ruminococcus luti*, *Ruminococcus productus* and *Ruminococcus schinkii* as *Blautia coccoides* gen. nov., comb. nov., *Blautia hansenii* comb. nov., *Blautia hydrogenotrophica* comb. nov., *Blautia luti* comb. nov., *Blautia producta* comb. nov., *Blautia schinkii* comb. nov. and description of *Blautia wexlerae* sp. nov., isolated from human faeces. *Int J Syst Evol Microbiol.* 2008; 58:1896–902. <https://doi.org/10.1099/ijs.0.65208-0> PMID:18676476
  65. Kasahara K, Krautkramer KA, Org E, Romano KA, Kerby RL, Vivas EI, Mehrabian M, Denu JM, Bäckhed F, Lusis AJ, Rey FE. Interactions between *Roseburia intestinalis* and diet modulate atherogenesis in a murine model. *Nat Microbiol.* 2018; 3:1461–71. <https://doi.org/10.1038/s41564-018-0272-x> PMID:30397344
  66. Jung TH, Park JH, Jeon WM, Han KS. Butyrate modulates bacterial adherence on LS174T human colorectal cells by stimulating mucin secretion and MAPK signaling pathway. *Nutr Res Pract.* 2015; 9:343–49.

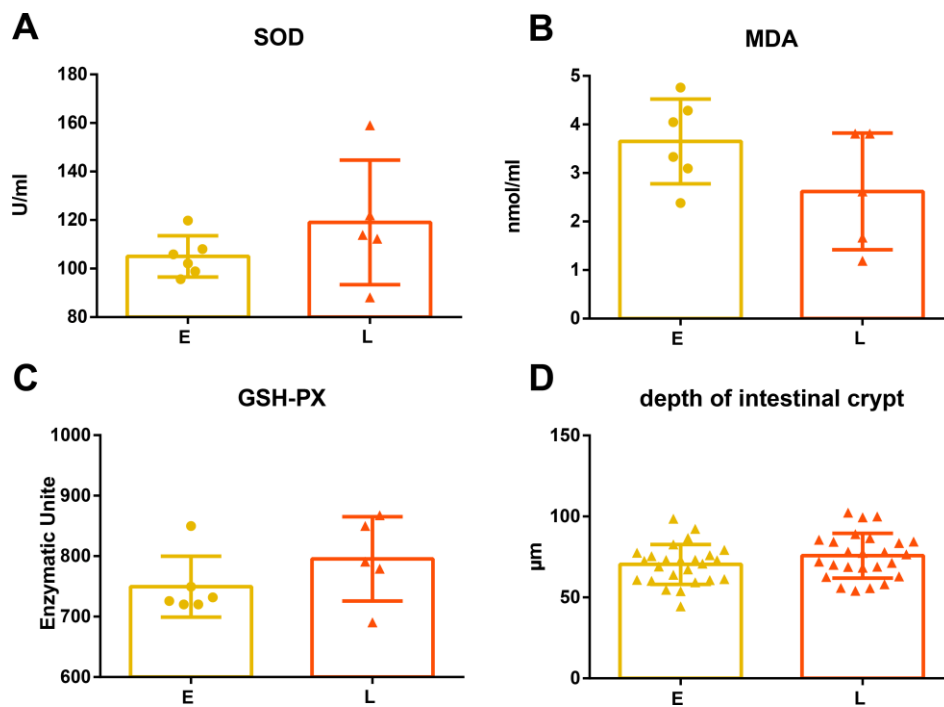


- <https://doi.org/10.4162/nrp.2015.9.4.343>  
PMID:[26244071](https://pubmed.ncbi.nlm.nih.gov/26244071/)
67. Shinagawa N, Iwasaki M. [Bacteria isolated from surgical infections and its susceptibilities to antimicrobial agents--Special references to bacteria isolated between July 1982 and March 2012]. *Jpn J Antibiot.* 2015; 68:151–87. PMID:[26349116](https://pubmed.ncbi.nlm.nih.gov/26349116/)
68. Feng Z, Long W, Hao B, Ding D, Ma X, Zhao L, Pang X. A human stool-derived *Bilophila wadsworthia* strain caused systemic inflammation in specific-pathogen-free mice. *Gut Pathog.* 2017; 9:59.  
<https://doi.org/10.1186/s13099-017-0208-7>  
PMID:[29090023](https://pubmed.ncbi.nlm.nih.gov/29090023/)
69. Natividad JM, Lamas B, Pham HP, Michel ML, Rainteau D, Bridonneau C, da Costa G, van Hylckama Vlieg J, Sovran B, Chamignon C, Planchais J, Richard ML, Langella P, et al. *Bilophila wadsworthia* aggravates high fat diet induced metabolic dysfunctions in mice. *Nat Commun.* 2018; 9:2802.  
<https://doi.org/10.1038/s41467-018-05249-7>  
PMID:[30022049](https://pubmed.ncbi.nlm.nih.gov/30022049/)
70. Alva-Murillo N, Ochoa-Zarzosa A, López-Meza JE. Short chain fatty acids (propionic and hexanoic) decrease *Staphylococcus aureus* internalization into bovine mammary epithelial cells and modulate antimicrobial peptide expression. *Vet Microbiol.* 2012; 155:324–31.  
<https://doi.org/10.1016/j.vetmic.2011.08.025>  
PMID:[21930351](https://pubmed.ncbi.nlm.nih.gov/21930351/)
71. Corr SC, Gahan CG, Hill C. Impact of selected *Lactobacillus* and *Bifidobacterium* species on *Listeria monocytogenes* infection and the mucosal immune response. *FEMS Immunol Med Microbiol.* 2007; 50:380–88.  
<https://doi.org/10.1111/j.1574-695X.2007.00264.x>  
PMID:[17537177](https://pubmed.ncbi.nlm.nih.gov/17537177/)
72. Claesson MJ, Cusack S, O'Sullivan O, Greene-Diniz R, de Weerd H, Flannery E, Marchesi JR, Falush D, Dinan T, Fitzgerald G, Stanton C, van Sinderen D, O'Connor M, et al. Composition, variability, and temporal stability of the intestinal microbiota of the elderly. *Proc Natl Acad Sci USA.* 2011 (Suppl 1); 108:4586–91.  
<https://doi.org/10.1073/pnas.1000097107>  
PMID:[20571116](https://pubmed.ncbi.nlm.nih.gov/20571116/)
73. Wu X, Sun R, Chen Y, Zheng X, Bai L, Lian Z, Wei H, Tian Z. Oral ampicillin inhibits liver regeneration by breaking hepatic innate immune tolerance normally maintained by gut commensal bacteria. *Hepatology.* 2015; 62:253–64.  
<https://doi.org/10.1002/hep.27791> PMID:[25783863](https://pubmed.ncbi.nlm.nih.gov/25783863/)
74. Turnbaugh PJ, Ridaura VK, Faith JJ, Rey FE, Knight R, Gordon JI. The effect of diet on the human gut microbiome: a metagenomic analysis in humanized gnotobiotic mice. *Sci Transl Med.* 2009; 1:6ra14.  
<https://doi.org/10.1126/scitranslmed.3000322>  
PMID:[20368178](https://pubmed.ncbi.nlm.nih.gov/20368178/)
75. Chunfu W, Qinghai Y, Wen L, Yueying G, Guiping Z. A study on the anti-aging effect of ginseng stem and leaf saponin in terms of the free radical theory of aging. *Journal of ShenYang college of pharmacy.* 1992:37–40.
76. Caporaso JG, Kuczynski J, Stombaugh J, Bittinger K, Bushman FD, Costello EK, Fierer N, Peña AG, Goodrich JK, Gordon JI, Huttley GA, Kelley ST, Knights D, et al. QIIME allows analysis of high-throughput community sequencing data. *Nat Methods.* 2010; 7:335–36.  
<https://doi.org/10.1038/nmeth.f.303> PMID:[20383131](https://pubmed.ncbi.nlm.nih.gov/20383131/)
77. Edgar RC, Haas BJ, Clemente JC, Quince C, Knight R. UCHIME improves sensitivity and speed of chimera detection. *Bioinformatics.* 2011; 27:2194–200.  
<https://doi.org/10.1093/bioinformatics/btr381>  
PMID:[21700674](https://pubmed.ncbi.nlm.nih.gov/21700674/)
78. Muyzer G, de Waal EC, Uitterlinden AG. Profiling of complex microbial populations by denaturing gradient gel electrophoresis analysis of polymerase chain reaction-amplified genes coding for 16S rRNA. *Appl Environ Microbiol.* 1993; 59:695–700.  
<https://doi.org/10.1128/AEM.59.3.695-700.1993>  
PMID:[7683183](https://pubmed.ncbi.nlm.nih.gov/7683183/)
79. Bartosch S, Fite A, Macfarlane GT, McMurdo ME. Characterization of bacterial communities in feces from healthy elderly volunteers and hospitalized elderly patients by using real-time PCR and effects of antibiotic treatment on the fecal microbiota. *Appl Environ Microbiol.* 2004; 70:3575–81.  
<https://doi.org/10.1128/AEM.70.6.3575-3581.2004>  
PMID:[15184159](https://pubmed.ncbi.nlm.nih.gov/15184159/)
80. Zeng B, Li G, Yuan J, Li W, Tang H, Wei H. Effects of age and strain on the microbiota colonization in an infant human flora-associated mouse model. *Curr Microbiol.* 2013; 67:313–21.  
<https://doi.org/10.1007/s00284-013-0360-3>  
PMID:[23604540](https://pubmed.ncbi.nlm.nih.gov/23604540/)

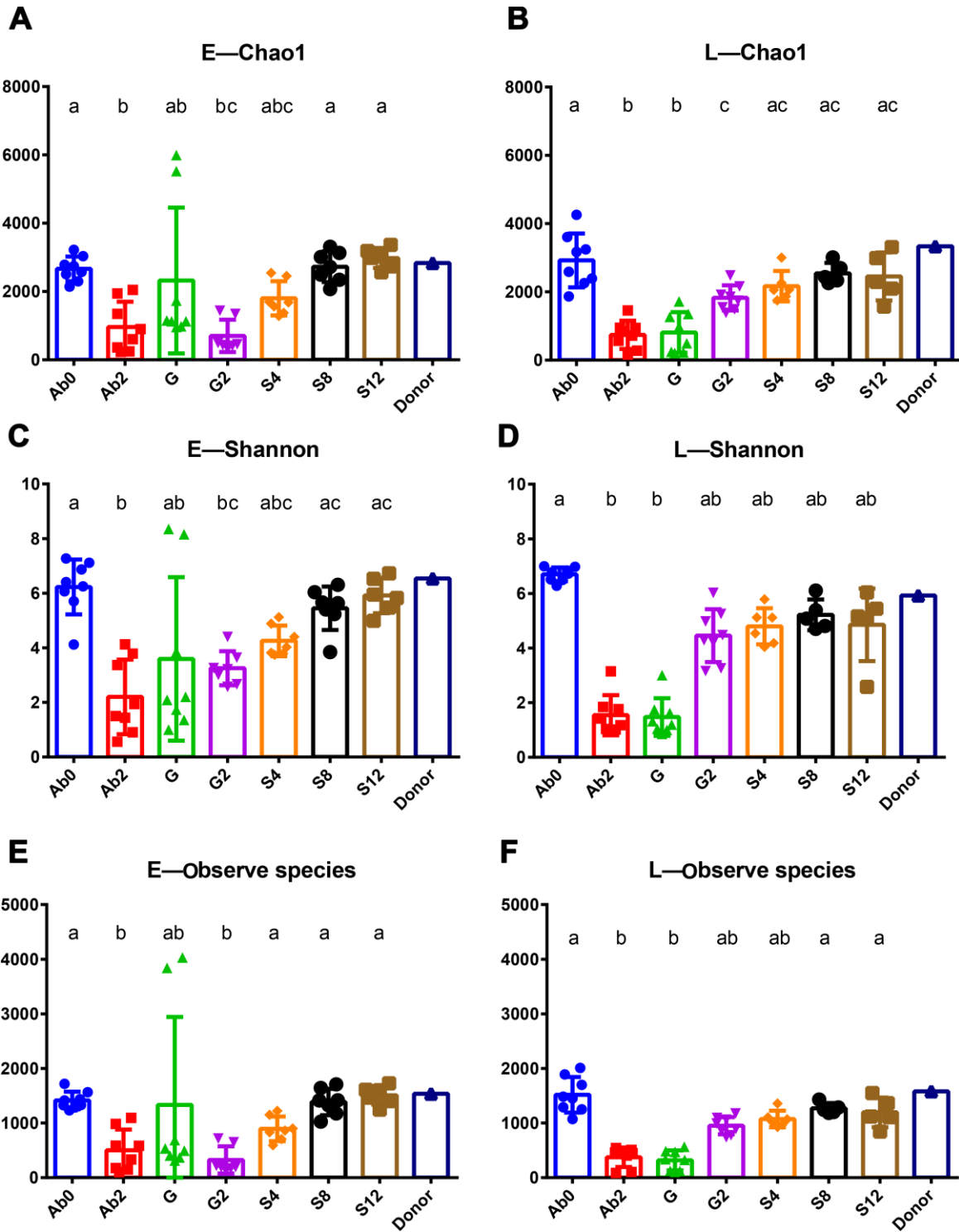


## SUPPLEMENTARY MATERIALS

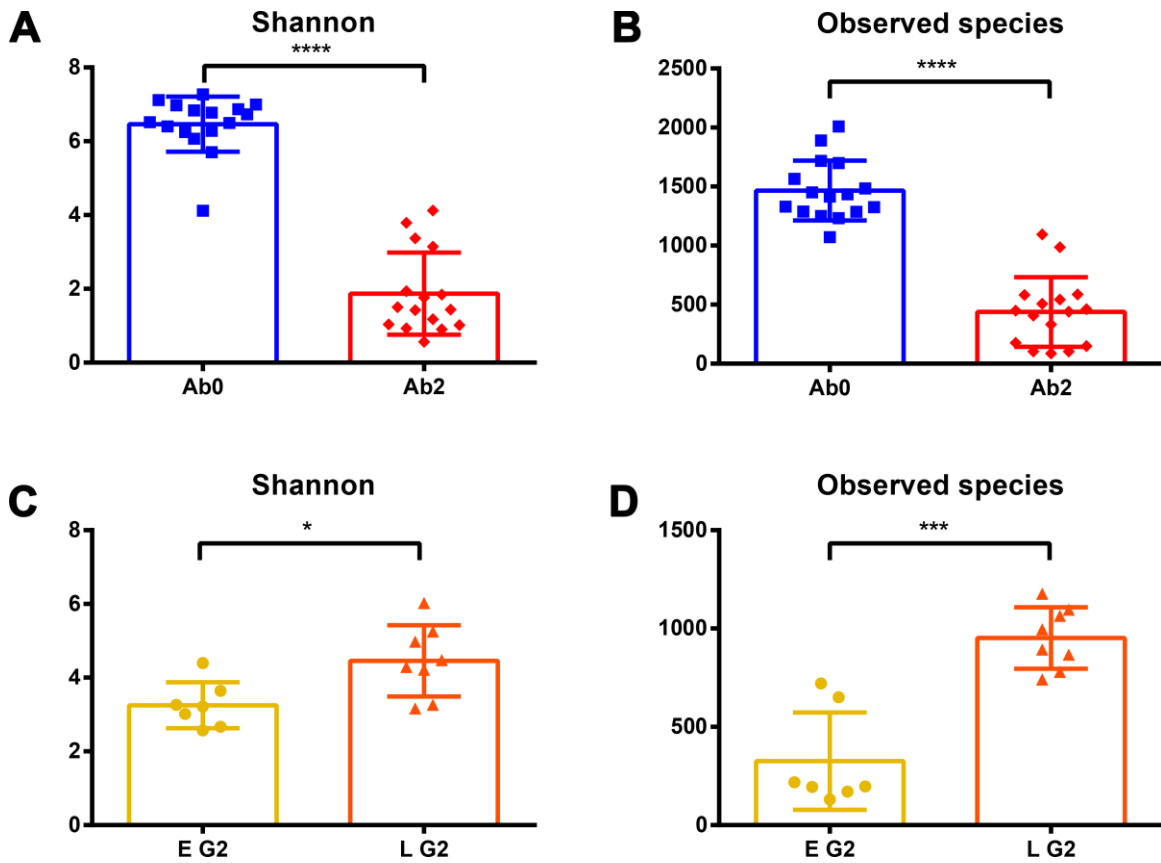
### Supplementary Figures



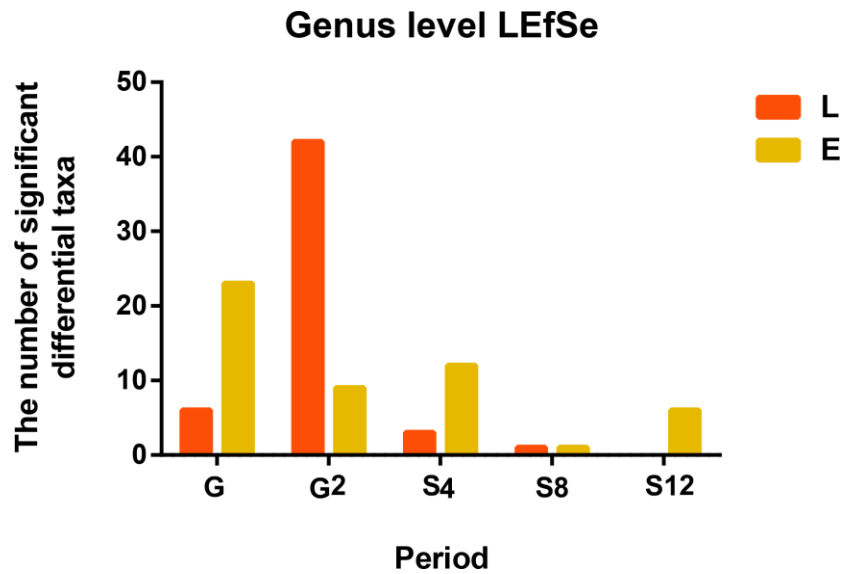
**Supplementary Figure 1. Antioxidant level in serum and depth of intestinal crypts.** (A) Superoxide dismutase (SOD), (B) malondialdehyde (MDA), (C) glutathione peroxidase (GSH-PX), (D) depth of intestinal crypt. Unpaired t test.



**Supplementary Figure 2. Alpha diversity in each period between groups.** Three metrics are shown, including (A, B) Chao1 index, (C, D) Shannon index, and (E, F) Observed species in both mice and donors. Dunn's multiple comparison test was used for multiple comparisons. Letters indicate inter-group significance. Lowercase letters represent  $p < 0.05$ .



Supplementary Figure 3. Comparison of the alpha diversity of the gut microbiome after antibiotic treatment. (A, C) Shannon diversity index. (B, D) number of observed OTUs. \* $p < 0.05$ , \*\*\* $p < 0.001$ , \*\*\*\* $p < 0.0001$ , Mann-Whitney U test.



Supplementary Figure 4. The number of significant differential taxa determined by LEfSe analysis at the genus level and OTU level. LDA cut off=2,  $p < 0.05$ .